Structural Study of Langmuir–Blodgett Mono- and Multilayers of Poly(β-hydroxybutyrate)

G. Lambeek, E. J. Vorenkamp, and A. J. Schouten*

Laboratory of Polymer Chemistry, University of Groningen, Nijenborgh 4, 9747 AG Groningen, The Netherlands

Received October 5, 1994; Revised Manuscript Received December 22, 1994[⊗]

ABSTRACT: In this study poly(β-hydroxybutyrate) (PHB) was used as a spreading material to form LB monolayers at the air–water interface. Isotherms were found to show a transition at about 14 mN/m that is argued to be associated with a phase transition in the monolayer. Stable monolayers could be obtained at various surface pressures before as well as beyond the transition. Multilayers on substrates were investigated with FT-infrared techniques and were shown to have crystalline characteristics. Hysteresis experiments confirm the occurrence of irreversible processes in the monolayer during compression. Transmission electron microscopy pictures clearly show the structural changes that appear with increasing stabilization surface pressure of the monolayer. At large areas PHB exhibits an expanded monolayer behavior. Under the influence of surface pressure PHB is argued to change into a crystalline structure and eventually to form a bilayer of helical molecules which is reflected in the shape of the isotherm. S-shaped stabilization curves are argued to be the result of an accelerated bilayer formation process, as is confirmed by TEM pictures of this layer. Infrared external reflection spectroscopy of a PHB monolayer on the water surface gives clear indications that PHB already crystallizes at the air–water interface during compression, thus confirming our theorem.

Introduction

Poly(β-hydroxybutyrate) (PHB) is an optically active aliphatic polyester produced by bacterial fermentation. Within the living organisms it occurs in a granular form[1] and serves as an energy and carbon storage product.[2,3] In that capacity it can be compared with glycogen in mammalian systems and starch in plants.

An important aspect of the research concerning PHB deals with the morphological differences between the polymer *in vivo* and the isolated polymer. Due to its natural origin, PHB has an exceptional stereochemical regularity which enables the polymer to crystallize. Research,[3,6] however, made it clear that PHB *in vivo* is in the amorphous state. The explanations postulated for this vary from the presence of water, responsible for keeping the core of the nascent granules in a noncrystalline state,[4] to pure crystallization kinetics of the submicrometric granules, which are dominated by homogeneous nucleation,[1] or the presence of some sort of plasticizer.[5,6] Crystallization is in any way induced by the various treatments that are a part of the isolation procedure.

Upon crystallization from the melt, the low level of heterogeneous nuclei present in the pure PHB, makes it a material very often used for model studies of polymer crystallization and morphology.[7] This resulted, for example, in the identification of five distinct types of nucleation in PHB[8] and the discovery of a class of nitrogen-containing nucleants.[9]

The crystal structure of isolated PHB consists of an orthorhombic unit cell $P2_12_12_1 - D_2^4$, with $a = 5.76$ Å, $b = 13.20$ Å, and c (fiber period) = 5.96 Å (corresponding with 2.98 Å/repeating unit). The unit cell contains two left-handed helical molecules in antiparallel orientation.[10] Furthermore there are reports on a paracrystalline structure of PHB. This concerns a strain-induced β-form of highly extended chains with a fiber period of 4.6 Å, corresponding to a twisted planar zigzag conformation.[11]

With the Langmuir film balance it is possible to study the behavior of a monolayer of PHB at the air–water interface. Previously, there have been several reports on the presence of polymers in helical conformations at the air–water interface.[12–17] This concerns helices already present in solution as well as helices formed upon compression of the monolayer at the air–water interface. Isotactic PMMA,[14,15] for example, exhibits an expanded coil conformation at large areas and changes into a helical conformation upon compression.

Taking stock of these results and considering the history of PHB research led to the question whether PHB (with its known helical crystalline structure) would under certain conditions also have a helical conformation at the air–water interface, either directly because of the presence of the helical conformation in solution or later under the influence of the applied pressure. Thus it seemed interesting to carry out an investigation into the behavior of PHB at the air–water interface. Besides the pressure–area isotherms and stabilization experiments that were carried out, infrared spectroscopy was performed at a monolayer on water by means of the external reflection technique. By this it is possible to obtain direct indications concerning the structure of PHB in the monolayer, in contrast with data acquired from layers on a substrate. These are always subject to possible changes caused by the transfer of the material onto the substrate. Finally, information concerning the monolayer structure was acquired with the use of transmission electron microscopy. Monolayers, stabilized at various surface pressures were examined and produced very useful information.

In addition to this study of monolayer properties, multilayers prepared with the Langmuir–Blodgett technique were examined. This technique has proven before to provide an opportunity to prepare thin films with a well-defined homogeneous thickness which may contain molecules in an ordered, sometimes crystalline,[12,18–22] structure with very distinct orientational characteristics. The orientation of molecules on substrates can often partly be ascribed to the LB depositing technique. Research namely has shown that during the transfer

[⊗] Abstract published in *Advance ACS Abstracts,* February 15, 1995.

0024-9297/95/2228-2023$09.00/0

of stiff polymer molecules or polymer crystals, a flow-induced orientation takes place. This alignment of molecules or crystals parallel to the dipping direction gives the film an anisotropic character.[23-25]

In this study research into these orientational effects as well as the structural characterization of the multilayers of PHB on various substrates was carried out with FT-infrared spectroscopy.

The techniques applied to the multilayers are transmission spectroscopy on IR-transparent substrates and external reflection (also called grazing incidence reflection or reflection absorption) spectroscopy on reflecting metal substrates. Grazing incidence IR spectroscopy reveals the orientation of the molecules with respect to the surface, since upon reflection on a metal surface, the resulting electrical field is strongly elliptically polarized, with only a significant contribution of the component perpendicular to the surface. Transmission IR spectroscopy performed with light polarized parallel or perpendicular to the dipping direction can elucidate the lateral orientation of the molecules on the substrate.

Experimental Section

Materials. The PHB used was a commercial Biopol sample provided by ICI Bioproducts & Fine Chemicals (Billingham, U.K.), M_w = 539K, M_w/M_n = 3.5, T_m = 176 °C.

LB. Monolayer properties were studied by using a computer-controlled Lauda Filmbalance FW2. The surface pressure could be measured with an accuracy of 0.05 mN/m. The subphase was water, purified by reverse osmosis and subsequent filtration through a Milli-Q purification system. The polymer was spread from chloroform solution (Uvasol quality, concentrations about 1 mg/mL). Pressure–area diagrams were measured at various speeds (1–10 Å^2/repeating unit/min) and various temperatures (5–25 °C). The compression was started at 50 Å^2/repeating unit.

Hysteresis experiments were carried out with a compression speed of 5 Å^2/repeating unit/min and a pause time of 10 min.

Transfer experiments were carried out after stabilization of the monolayer at constant temperature and surface pressure. Substrates were ZnS and gold-sputtered glass slides. ZnS plates were ultrasonically cleaned with organic solvents. Gold substrates were prepared by sputtering gold (thickness approximately 500 Å) onto glass slides with a Biorad Turbo-coater E6700. Dipping speeds were 4 mm/min downward and 1 mm/min upward at a temperature of 20 °C.

IR. Infrared measurements were carried out with a Mattson Galaxy 6021 FT-IR spectrometer and a Bruker IFS88 FTIR spectrometer both equipped with a MCT-A detector (D-313, Infrared Associates). The spectra were recorded with a resolution of 4 cm^{-1} unless mentioned otherwise. All reported spectra were baseline corrected. A germanium Brewster angle IR polarizer was used for both reflection and transmission experiments.

Grazing incidence reflection spectra were recorded in the Bruker spectrometer in a 80° specular setup with light polarized parallel to the plane of incidence. The spectra were taken from part of the gold substrate, which was covered with LB multilayers, and referenced against a clean part of the same substrate. Transmission spectra with polarized radiation (0° and 90°) were obtained under a small tilt in order to avoid the internal reflections within the ZnS substrate. Transmission spectra of the clean substrate were used as a reference for these spectra.

Temperature dependent IR spectroscopy was performed on solution cast films of PHB on silicon in a Mettler hot stage in the Bruker spectrometer. Thicknesses of these films were measured with a Sloan Dektak 3030ST.

External reflection spectroscopy of monolayers on water was performed with the use of a Specac monolayer/grazing angle accessory (P/N 19650 series) in the Mattson spectrometer. The reflection angle was 45°. Light was polarized perpendicularly to the plane of incidence. The spectra were recorded with a resolution of 8 cm^{-1} and 2000 scans were taken. An external reflection spectrum of the clean water surface was used as a reference for the spectra.

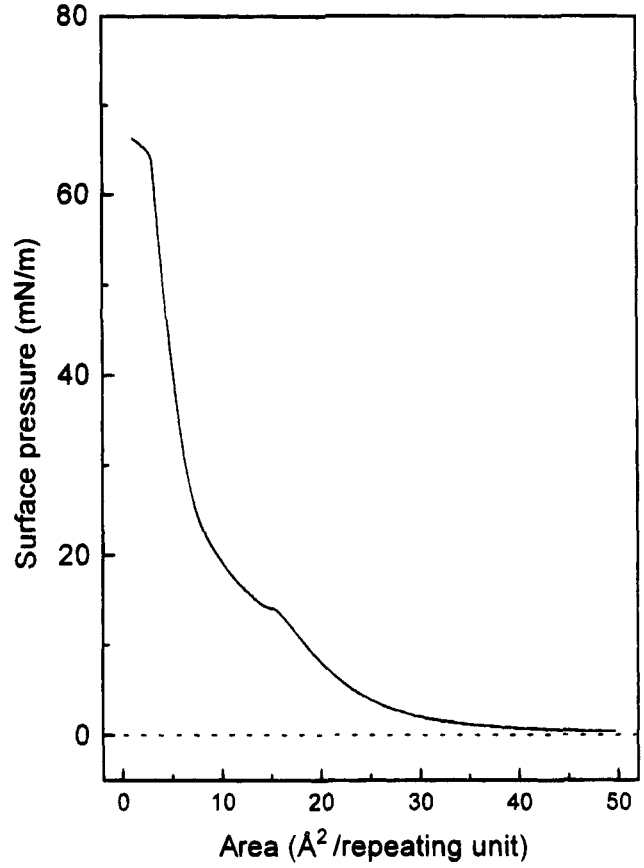

Figure 1. Pressure–area isotherm of PHB. Compression speed 5 Å^2/repeating unit/min, T = 20 °C.

Unfortunately, it was not possible to simultaneously perform surface pressure measurements. The amount of PHB applied (chloroform solution, Uvasol quality, concentration 0.1456 mg/mL) and the surface area of the trough in the monolayer accessory were determined as exact as possible. Since these measurements were carried out at 20 °C, the pressure–area isotherm of Figure 1 could now be used to determine quite accurately in which part of the isotherm we were measuring.

Spectral Simulations. Reflection spectra of thin films deposited on different substrates are generally modified by optical effects. Distinguishing the changes observed in reflection spectra caused by these optical effects is crucial for the interpretation of the spectroscopic data and must be done before relating any differences in band shape, position, and intensity to structural, orientational, and/or chemical bonding changes in the film. Therefore, spectral simulation has been used to eliminate the influence of these optical effects and to make a comparison of the various spectra possible.[15,27]

The optical constants of PHB necessary for the spectral simulations were calculated according to the following procedure. A transmission spectrum of bulk crystalline PHB powdered with KBr was used as an input spectrum. The amount of material was estimated by assuming that the PHB was present as a film on a KBr substrate. The thickness of this film and the refractive index n of the PHB were estimated. For all PHB samples the real part of the refractive index was centered[15] at 1.45. The absorption coefficients were converted into k values after which the n-spectrum can be calculated from the estimated k-spectrum with the Kramers–Kronig relationship.[15] On the basis of the optical constants acquired in this way a spectrum of a film of PHB on silicon was calculated and compared to an experimental input spectrum of a solution cast film of PHB on silicon with a known thickness. Adjusting the thickness of the original KBr spectrum several times finally gave a good reproduction of experimental spectra of films on silicon for various thicknesses. For the optical constants of the substrates values were used for the complex refractive indices of 9.5–30i for gold, 3.8 for Si,

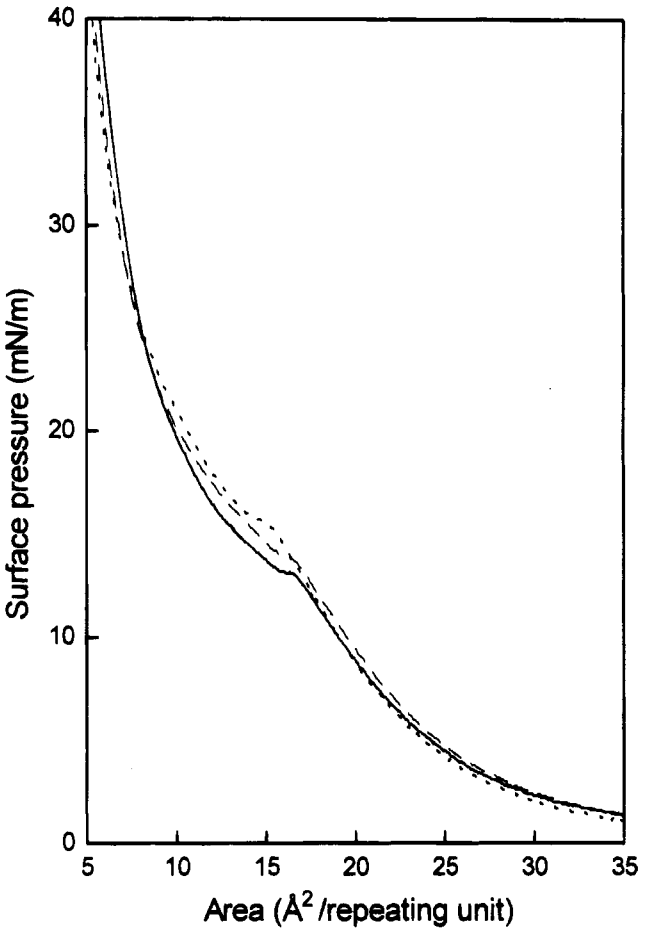

Figure 2. Pressure–area isotherms of PHB. T = 20 °C, compression speed 1 (—), 5 (- - -), and 10 (• • •) Å²/repeating unit/min.

and 2.22 for ZnS.[37] For water values of n = 1.241 and k = 0.0441 were used.[27]

Transmission Electron Microscopy. Samples for the electron microscope were prepared by using a manual horizontal lifting method with a carbon-coated grid as the substrate. The specimens were blotted dry by touching the edge of the grid with filter paper and were subsequently shadowed with platinum at an angle of 20°. The electron micrographs were recorded on a Philips 300 EM microscope at 80 kV using a magnification of 27 000 times. Transmission electron microscopy (TEM) was performed on monolayers stabilized at various surface pressures.

Results and Discussion

The only authors before to report on the monolayer behavior of PHB were G. A. R. Nobes, D. A. Holden, and R. H. Marchessault.[28] They observed an increase of surface pressure without obvious collapse points up to a maximum of 20 mN/m at areas of about 12 Å²/repeating unit. This maximum appears to be chosen quite arbitrarily in view of the pressure–area isotherm presented in Figure 1. The above mentioned maximum surface pressure now appears to be merely a point somewhat beyond a "transition" in the isotherm. This transition occurs in the pressure–area isotherm of PHB at every temperature and compression speed utilized in this investigation. In our opinion this transition should not be considered to be the maximum pressure, as will be discussed later on.

From the effect of compression rate on the shape of the isotherms and the position of the transition, more information can be deduced about the nature of the process (Figure 2). The trend found here is that the pressure at which the transition takes place increases with increasing compression rate. At the smallest compression rate the transition is also shifted somewhat toward smaller areas per repeating unit. Apparently, the transition in the isotherms is associated with a rather slow process.

Another part of the isotherm that gives information about PHB is the low-pressure part. It shows that a pressure of about 0.7 mN/m can be measured even at areas of 50 Å²/repeating unit. This kind of behavior is typical for an expanded monolayer. This effect has previously been described for several polymers such as isotactic poly(methyl methacrylate) (PMMA),[14] poly(*n*-butyl methacrylate) (PnBMA), and poly(vinyl acetate) (PVAc).[29] Cohesive forces between segments of the polymer chain have been argued to play an important role in this behavior.

For PHB this can be explained as follows. The ester groups of PHB might be oriented favorably with respect to the water subphase like an amphiphilic molecule, while the hydrophobic part of the polymer is oriented toward the air side. The ester groups are now pointing more or less downward, which results in a repulsive effect of the dipoles. Another effect that occurs is the screening of the dipolar interactions between the ester groups laterally, diminishing the dipolar interactions and thus the lateral cohesive forces between the chains. Sequences of these oriented segments can be argued to induce and stabilize the orientation of the individual segments, since they cannot move independently from each other.

This expanded monolayer behavior does not agree with the model proposed by G. A. R. Nobes et al.[28] They argued that at the air–water interface PHB is present in the paracrystalline β-structure. They proposed a structure that matches the model concerning hydrogen-bonded water molecules between adjacent portions of growing polyalkanoate chains during biosynthesis.[4] In our opinion, the limitation of molecular movement in this crystalline state would inhibit the monolayer from building up a small surface pressure at large areas. To explain the expanded monolayer behavior, we therefore must conclude that a major part of the molecules is present in a noncrystalline conformation.

Stabilization and Transfer

Figure 3 shows the results of stabilization experiments performed at different surface pressures. Stable layers could be obtained over a range of pressures before as well as beyond the pressure corresponding with the transition in the isotherm. The areas per repeating unit at which the monolayer stabilizes are in good agreement with the surface pressure–area isotherms. This proves that the process associated with the transition in the isotherm is not some kind of collapse process because in that case stable layers would not be expected let alone layers with an area per repeating unit in good agreement with the pressure–area isotherms. Moreover, this proves that great surface pressure gradients are absent in PHB monolayers in spite of the high molecular weight material.

Monolayers stabilized at 9 or 11 mN/m were transferred onto ZnS and gold with the use of the vertical LB dipping technique. Transfer ratios are listed in Table 1. Unfortunately, no appreciable transfer could be obtained at surface pressures above the transition, so no direct information about the generated structure could be acquired.

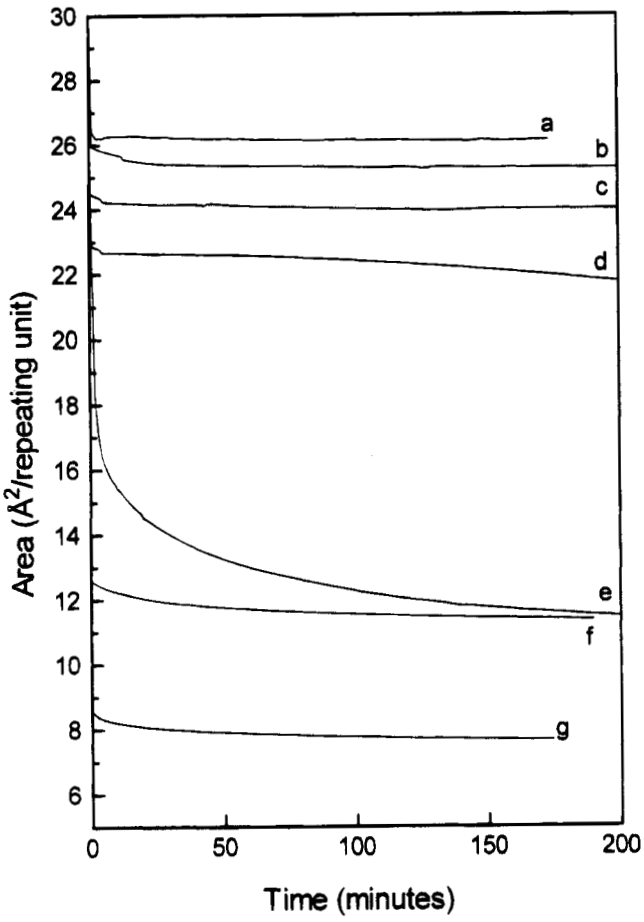

Figure 3. Stabilization curves of PHB at 8 (a), 9 (b), 11 (c), 13 (d), 15 (e), 20 (f), and 30 (g) mN/m.

Table 1. Transfer Ratios of PHB[a]

pressure (mN/m)	transfer up	transfer down
9	0.8	0
11	0.7	0

[a] Temperature 20 °C; dipping speed 4 mm/min downward, 1 mm/min upward.

IR of Multilayers

An IR study of the above mentioned multilayers of PHB was performed. To our knowledge no detailed vibrational analysis of PHB has appeared in the literature yet. Band assignments had to be made by combining the results of other components.[30-35] The assignments of the most important bands are given in Table 2.

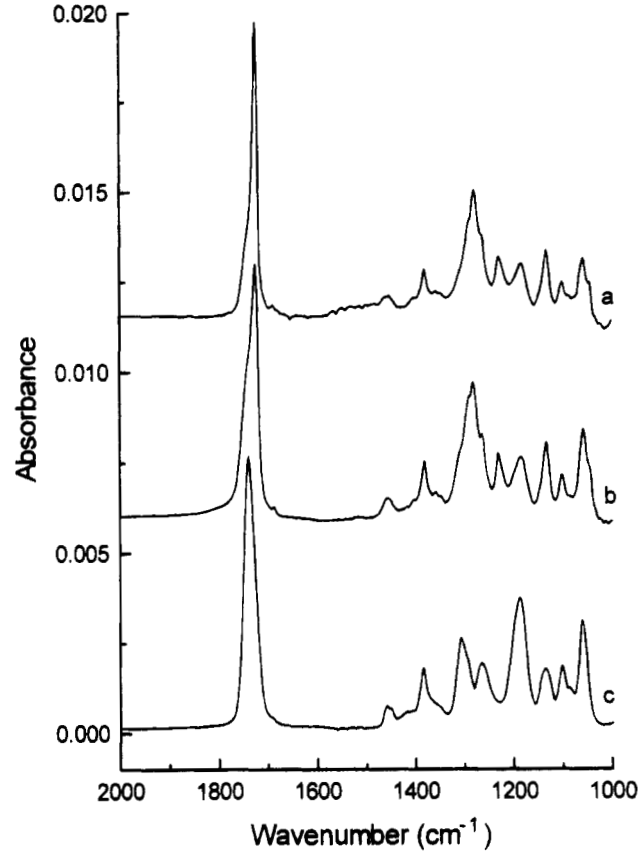

Figure 4. IR spectra of PHB. Transmission spectrum of LB layers on ZnS transferred at a surface pressure of 9 mN/m (a), PHB bulk powdered with KBr (b), and PHB in solution in $CDCl_3$ (c).

We carried out transmission experiments with multilayers transferred onto IR-transparent substrates (ZnS). The transmission spectrum of Langmuir–Blodgett layers of PHB transferred at a surface pressure of 9 mN/m is shown in Figure 4a. The other spectra in this figure represent respectively bulk PHB powdered with KBr (Figure 4b) and PHB in $CHCl_3$ solution

Table 2. Assignments of IR Absorption Bands of PHB[19-22,30-32,35]

wavenumber (cm^{-1})	assignment[19,21,22,30-32,35]	dipole transition moment[19,35]
3005	$\nu_a(CH_3)$ out of/in skeletal plane	
2996	$\nu_a(CH_3)$ in/out of skeletal plane	
2986	$\nu_s(CH_3)$	∥ to C–CH_3 bond, in Fermi resonance with overtone at 2955 cm^{-1}
2977	$\nu_a(CH_2)$	⊥ to CCC chain plane
2955	$\nu_s(CH_3)$	∥ to C–CH_3 bond, in Fermi resonance with $\nu_s(CH_3)$ at 2986 cm^{-1}
2934	$\nu_s(CH_2)$	∥ to H–C–H plane, bisecting the HCH angle
2890	$\nu_a(CH)$	⊥ to CCC chain plane
1739	$\nu(C{=}O)$	∥ to C=O bond
1724	$\nu(C{=}O)$	∥ to C=O bond
1458	$\delta(CH_2)$	∥ to H–C–H plane, bisecting the HCH angle
1449	$\delta_{as}(CH_3)$	⊥ to C–CH_3 bond
1380	$\delta_s(CH_3)$	∥ to C–CH_3 bond
1290		
1278	crystal vib	
1263		
1231	wag & twist CH_2	
1183	$\nu_a(COC)$	
1133	$\nu_s(COC)$	
1101		
1086	butyrates other bands	
1058	butyrates other bands	
1049		
980		

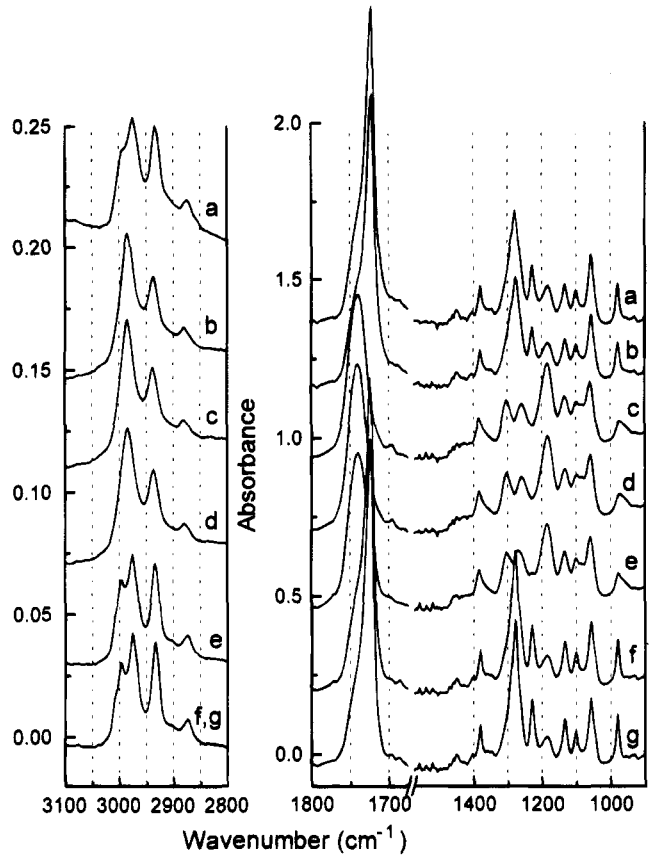

Figure 5. Transmission spectra of solution cast PHB on silicon: starting temperature 100 °C (a), heated to 150 °C (b), 175 °C (c), after 10 min at 175 °C (d), cooling to 150 °C (e), 100 °C (f), and 75 °C (g).

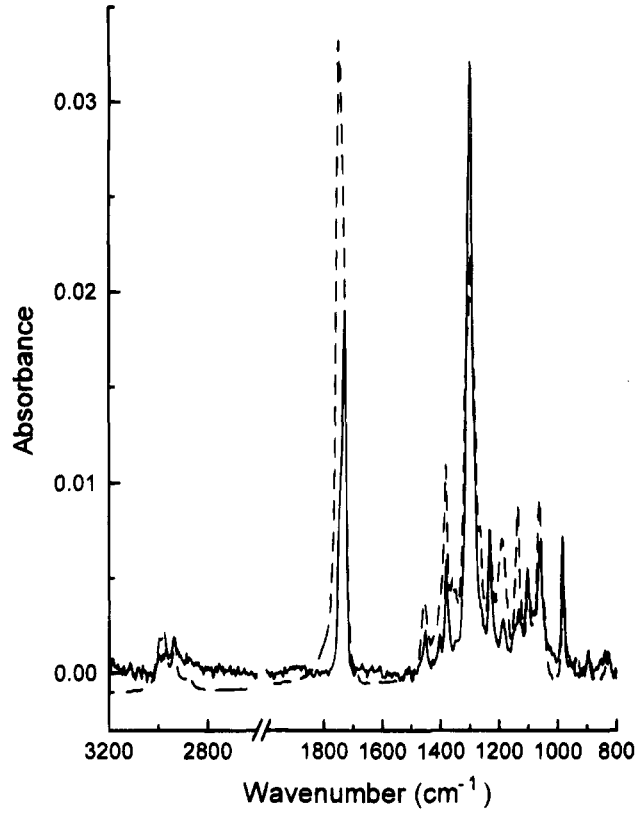

Figure 6. GIR spectrum of LB layers of PHB transferred on gold at a surface pressure of 11 mN/m (—) and calculated GIR spectrum of crystalline nonoriented PHB on gold (- - -), details in the Experimental Section.

(Figure 4c). When we compare these two spectra we can see some striking differences between the dissolved and crystalline PHB. When we now compare these spectra with each other on the one side and with the transmission spectrum of LB multilayers on the other side, a preliminary conclusion might be drawn that the multilayer spectrum bears more resemblance to the spectrum of crystalline PHB than to the spectrum of dissolved PHB.

To get a better overall picture of the spectral differences between amorphous and crystalline PHB, we heated a sample of solution cast PHB on silicon and simultaneously recorded transmission spectra. These series of spectra are shown in Figure 5. Striking differences are seen in the bands at 1185, 1228, and 1279 cm^{-1}, which were reported before to be crystallinity-sensitive.[26] In a spectrum of crystalline PHB the bands at 1228 and 1279 cm^{-1} are very distinctly present, whereas they are not present at all in the spectrum of amorphous PHB. On the contrary, the band at 1185 cm^{-1} appears during heating of the sample and is therefore characteristic for amorphous PHB. However, these are not the only bands to be influenced by a change in crystallinity. The C=O stretching vibration at 1724 cm^{-1} is shifted toward higher frequency as the temperature is raised to 175 °C. Although there is already a shoulder present at the high-frequency side of the 1724 cm^{-1} band in the spectrum of crystalline PHB, the intensity of this band increases considerably during heating while the intensity of the 1724 cm^{-1} band decreases similarly. Another difference is seen in the C—H stretching region. The $\nu_a(CH_2)$ band at 2977 cm^{-1} increases considerably in intensity and shifts toward higher frequency, thereby overlapping the ν_s and ν_{as} of CH_3. This frequency shift is also reported for LB layers of cadmium arachidate[30] and is indicative of the packing density reduction which occurs in the melt phase.

The PHB recrystallizes during cooling and exhibits the same spectrum as before the procedure, as can be seen in Figure 5f,g. The 1228 and 1279 cm^{-1} bands are clearly present whereas the band at 1185 cm^{-1} is not present at all. Furthermore, the C=O stretching vibration occurs at 1724 cm^{-1} with a shoulder at the high-frequency side, which is also indicative of crystalline material. The intensity of the bands in the C—H stretching region leads to the same conclusion that the material present on the substrate is most likely to be crystalline. Summarizing, we may conclude that the transmission spectra of the LB layers of PHB on ZnS in Figure 4 have all the characteristics of a crystalline sample.

Assuming that the PHB on the substrate is crystalline rendered the opportunity to use spectral simulations to make further interpretations of the experimental spectra possible. (See Experimental Section for more details.) It was now possible to calculate the spectra that would be found when nonoriented crystalline material was to be present on the various substrates. Any differences between the calculated and the experimental spectrum of crystalline material can then be ascribed to orientation of material on the substrate.

LB Multilayers. The grazing incidence reflection spectrum of Langmuir–Blodgett layers of PHB, transferred at a surface pressure of 11 mN/m, is shown in Figure 6, together with a simulated grazing incidence reflection spectrum of a film of crystalline nonoriented PHB on gold with a thickness of 50 nm (more details in the Experimental Section). When we compare these two spectra, significant differences can be seen. A major difference emerges in the intensity of the C=O stretch-

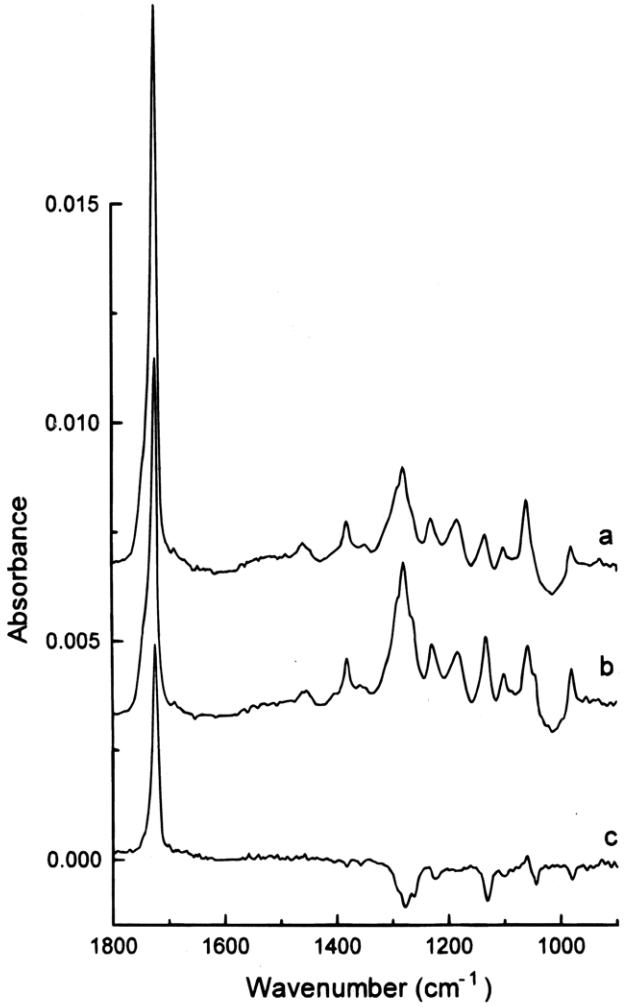

Figure 7. Polarized transmission spectra of an LB layer of PHB transferred on ZnS at a surface pressure of 9 mN/m and the difference spectrum. Polarization perpendicular to the dipping direction (a), parallel to the dipping direction (b), difference spectrum (=(a) − (b)) (c).

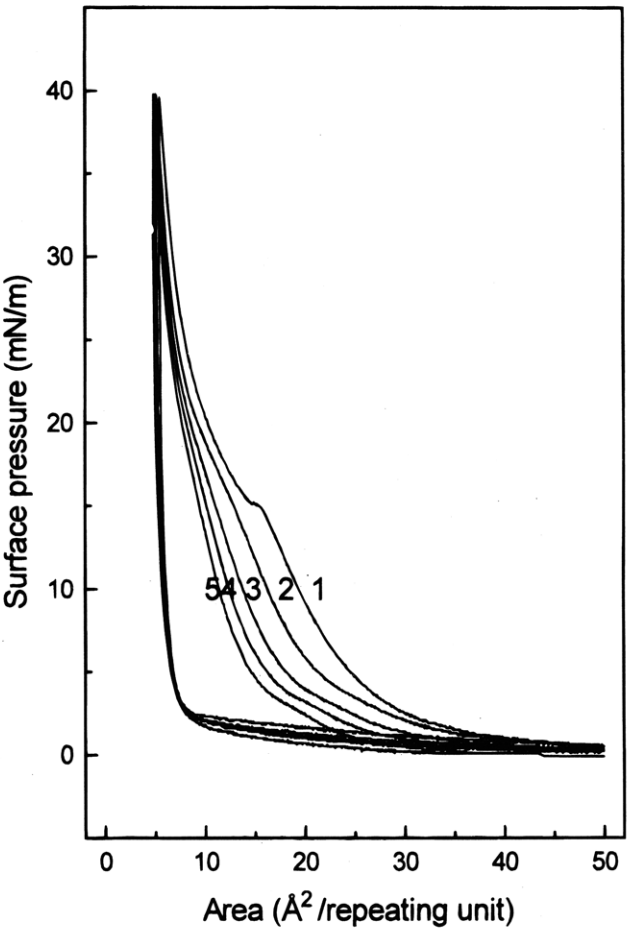

Figure 8. Five subsequent hysteresis isotherms of PHB. Compression speed 5 Å²/repeating unit/min, pause time 10 min, $T = 20$ °C.

ing vibration (1724 cm^{-1}). The experimentally found intensity is much smaller than the calculated intensity for a nonoriented crystalline film. This indicates that on average the transition dipole moment of this vibration has a smaller component perpendicular to the substrate than would be expected for a nonoriented crystalline film. Since the dipole transition moment of this vibration lies parallel to the C=O bond, this bond

Chart 1. Proposed Orientation of Crystalline PHB at the Air–Water Interface, Based on the Crystal Structure of Naturally Occurring Optically Active Poly(β-hydroxybutyrate)[10,a]

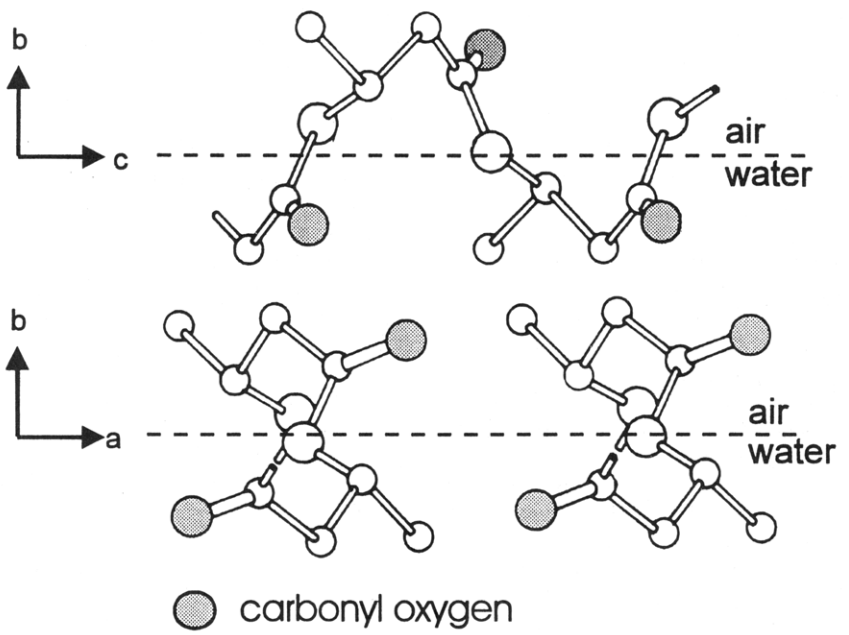

[a] The axes shown correspond with the axes of the PHB unit cell as described in ref 10.

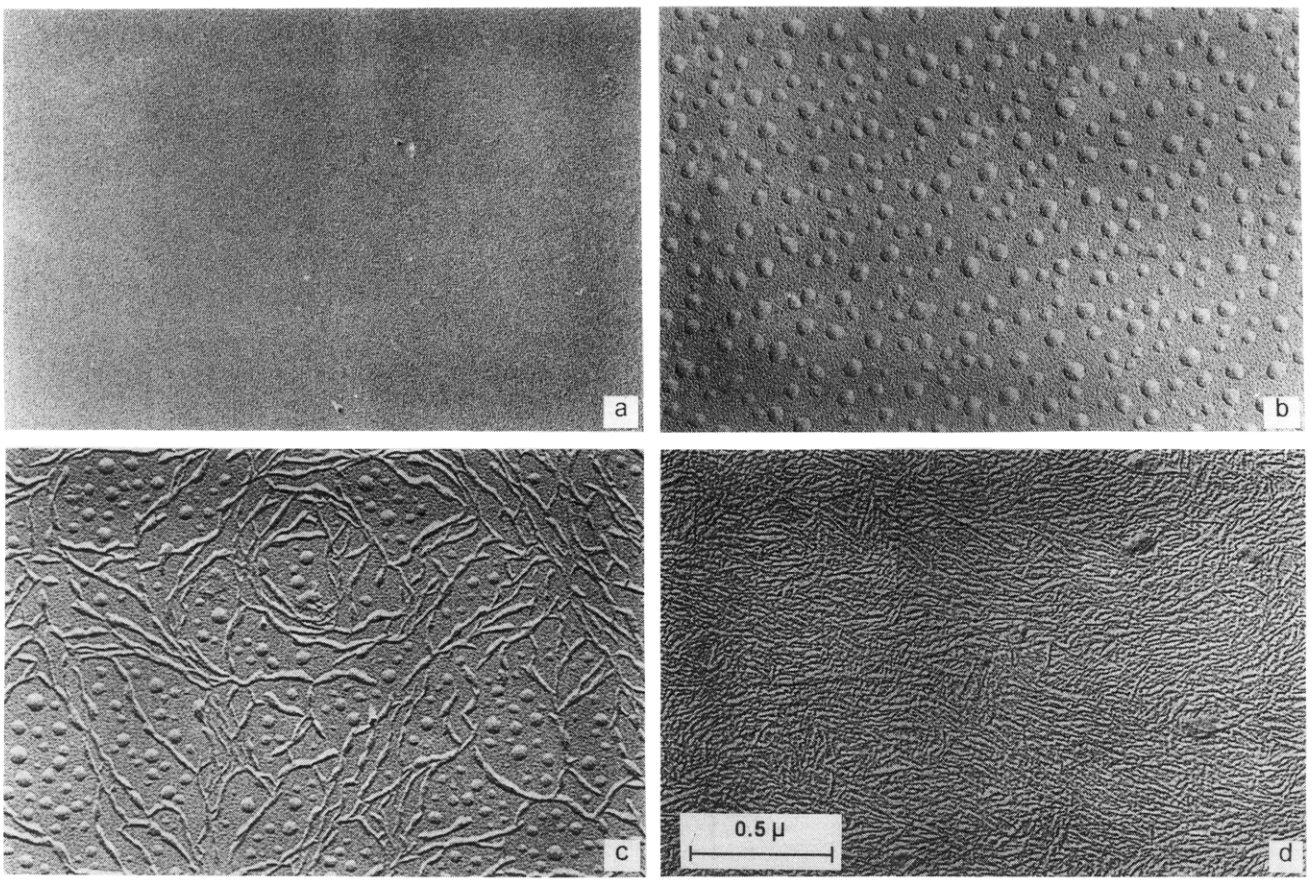

Figure 9. TEM pictures of PHB at the air–water interface. Temperature 20 °C. Stabilization surface pressure: 0.6 (a), 5 (b), 9 (c), and 20 mN/m (d).

is predominantly oriented parallelly to the surface. Furthermore, strong orientational effects can be seen looking at $\delta_s(CH_3)$ at 1380 cm^{-1}. It shows a decreased absorption intensity in the experimental spectrum compared to the calculated spectrum. Knowing that the dipole transition moment of this vibration is oriented parallel to the C—CH_3 bond, we may conclude that this bond is oriented parallel to the substrate.

Furthermore we carried out transmission experiments with multilayers transferred onto IR-transparent substrates (ZnS). This allowed the film to be probed by an electrical field parallel to the substrate. By using polarized light, it is possible to make a distinction between the dipping direction and the direction perpendicular to it. Comparison of the two transmission spectra of multilayers of PHB on ZnS was done by subtracting the two spectra from each other. Figure 7 shows the two transmission spectra and their difference spectrum. A striking effect is seen in the intensity of the C=O stretching vibration at 1724 cm^{-1}. Since the dipole transition moment of this vibration is parallel to the C=O bond, the orientation of this bond is preferentially perpendicular to the dipping direction. Another striking difference emerges in the $\nu_s(COC)$ band at 1133 cm^{-1}, which clearly has a larger intensity parallel to the dipping direction. The same applies to the 1278 cm^{-1} crystal vibration, which cannot be assigned to a specific vibration and thus will not help in elucidating the orientation of the structure. This also holds for the bands below 1300 cm^{-1}, which show some orientational effects but cannot be assigned unambiguously because of the complexity of coupled vibration modes.

Summarizing, we found that the C=O bond is oriented parallel to the substrate surface and perpendicular to the dipping direction. The C—CH_3 bond is also oriented parallel to the substrate surface.

If it is assumed that the PHB is present at the substrate in the helical conformation, the orientations of the C=O and C—CH_3 bonds indicate that these helices must be oriented parallel to the dipping direction. The bonds are more or less pointing out of the helix perpendicular to the helix axis. This kind of orientation of helical structures in the transfer direction is reported before by several authors.[15–17] It indicates that the helical structures are already present at the air–water interface or are formed during transfer because in those ways the flow caused by the transfer process can induce the helical orientation parallel to the dipping direction. Chart 1 shows a proposed orientation of the crystalline PHB at the air–water interface that is in good accordance with these bond orientations.

Hysteresis

Hysteresis experiments might give indications whether or not irreversible changes of the monolayer structure take place during compression. Hysteresis experiments performed with a maximum pressure before the transition in the isotherm showed that no considerable irreversible changes have occurred during compression. The subsequent cycles show a negligible decrease of the area per repeating unit at the maximum surface pressure. Hysteresis experiments with a maximum surface pressure beyond the transition in the isotherm show that under the influence of the increased surface pressure irreversible changes in the monolayer have occurred. Figure 8 shows that the monolayer changed considerably during the first cycle. The decompression curve does not follow the compression curve: the pressure drops sharply in the pause before decompression and during decompression eventually approaches the compression isotherm at large areas. Recompression of the same monolayer clearly shows the irrevers-

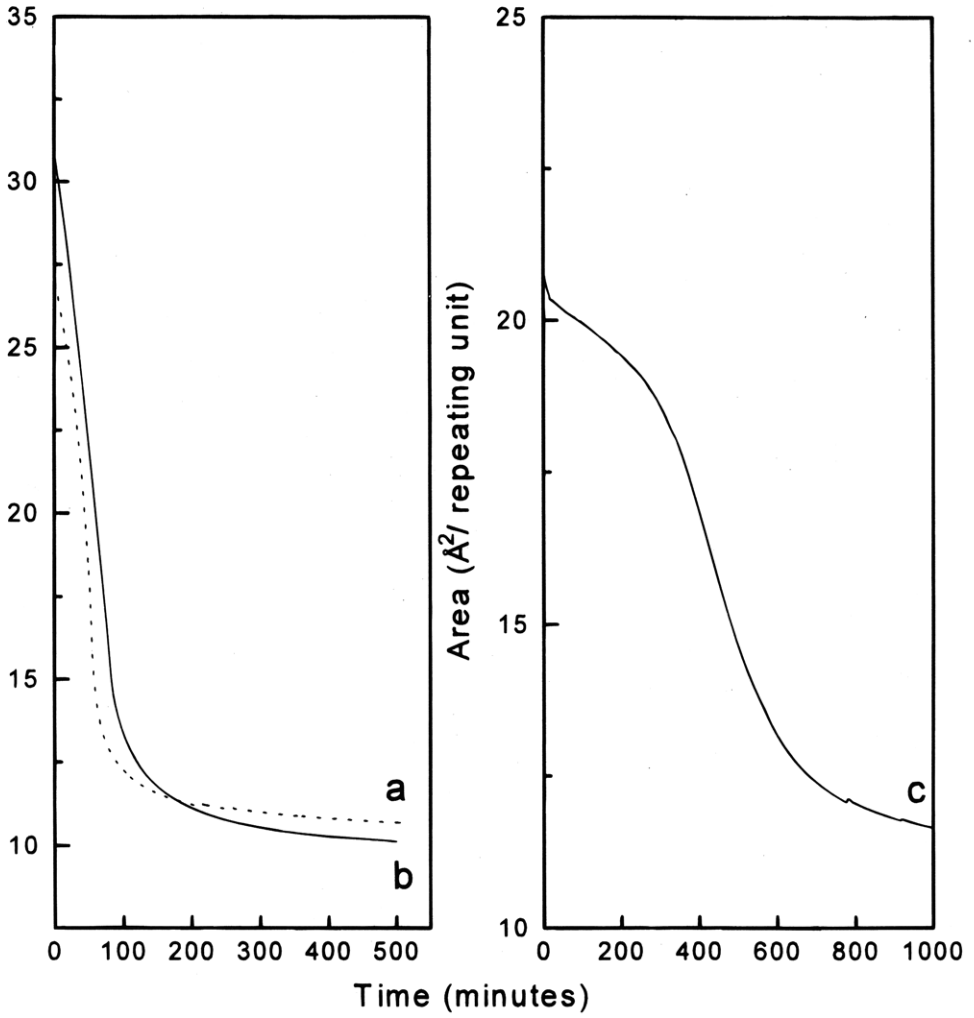

Figure 10. Stabilization curves of PHB. Temperature 20 °C. Surface pressure: 7.5 (a), 6 (b), and 9 (c) mN/m.

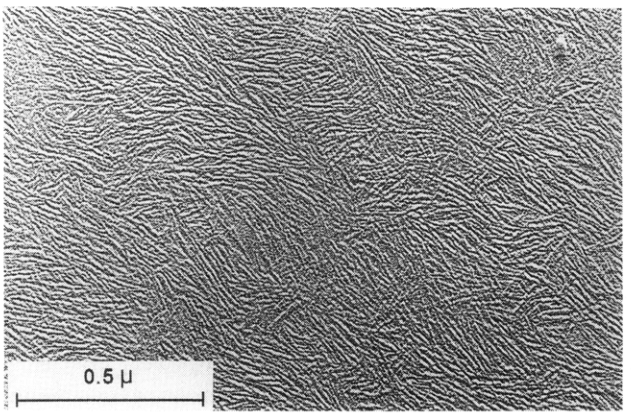

Figure 11. TEM picture of PHB at the air–water interface. Temperature 20 °C, stabilization surface pressure 9 mN/m, S-shaped stabilization curve.

ible changes. The transition expected to occur at compression beyond the corresponding point in the isotherm does not take place at all. Evidently, even at very small pressures the structures that formed did not decompose completely. On this time scale the formed structures do not "melt" at surface pressures comparable to those at which they were formed.

In addition to the disappearance of the transition in the isotherm, the surface pressure at a specific area per repeating unit simultaneously drops significantly. Apparently, the monolayer attains a higher degree of conversion than in the first run. This process can be repeated a number of times, each new cycle leading to a slightly higher degree of conversion. Thus during several subsequent compression/decompression cycles the surface pressure associated with a constant area per repeating unit decreases constantly. This may be explained by a loss of mobility which keeps the nonconverted polymer chains from converting. Upon decompression these immobilizing constraints may be partially lost, allowing for some reorganization. During the next compression a higher degree of conversion can be reached, a process that can be repeated several times. The experiment shows that the changes occurring in the monolayer during compression are irreversible and structures are formed that grow and pack more tightly during each cycle.

Transmission Electron Microscopy (TEM)

Figure 9 shows several TEM pictures in order of increasing stabilization surface pressure. It can be seen clearly that at low pressure a monolayer is obtained which is predominantly homogeneous without any appreciable structures. With increasing surface pressure we see that small parts of the monolayer start to form small domains of comparable size, shape, and thickness which are somewhat thicker than the surrounding monolayer. At 9 mN/m a part of the domains starts to stick together and form ribs that are thicker than the original domains. Another part of them still maintains their separate structures. Figure 9d shows the TEM picture of the layer stabilized at 20 mN/m. Almost all

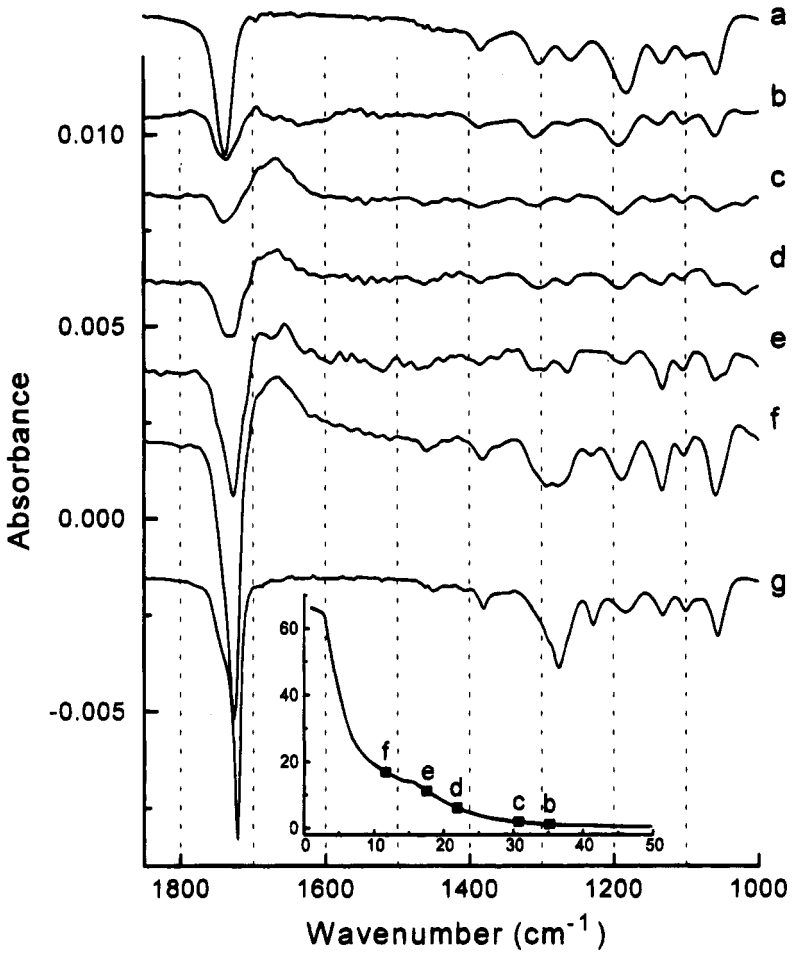

Figure 12. Reflection absorption IR spectra of PHB at the air–water interface. Calculated spectra of an amorphous (a) and a crystalline (g) film of PHB of 1 nm thickness (details in the Experimental Section). Experimental spectra of PHB, area per repeating unit: 35.2 Å^2 (b), 30.8 Å^2 (c), 22 Å^2 (d), 17.6 Å^2 (e), and 11.7 Å^2 (f).

domains formed ribs which in their turn formed connections between one another. In this way finer structures have developed which are packed more closely.

Indications concerning the nature of the formed structure can be found when we extrapolate the linear post-transitional region of the isotherms to zero pressure. A specific area of approximately 10 Å^2/repeating unit is obtained in that case. On the basis of the average surface area of the *ab* and *bc* faces of the PHB unit cell of the 2_1 helical crystalline structure, a packing density of 17.2 Å^2/repeating unit is calculated (see Chart 1). So the measured value of 10 Å^2 approximately matches twice the value of the extrapolated post-transitional region and thus is indicative of the formation of a bilayer, as was suggested before by Malcolm for synthetic polypeptides.[13] He argued that the plateau or inflection in a pressure–area isotherm represents the region where molecules leave the water surface and start to form a second layer in a regular manner. The mechanism he proposed starts from a number of molecules in the monolayer under pressure that are forced out of the lower layer and act as nuclei for the formation of the second layer. Once this has happened, the second layer will be formed as a co-operative process in which lower layer molecules are forced into the upper layer because of attractive forces between the layers. In our view the process occurring during compression can now be summarized as follows.

At large areas the PHB monolayer is predominantly in an expanded conformation and thus exhibits a small pressure. When the (stabilization) surface pressure is increased, a few molecules act as nucleants for surrounding molecules to form helices, thus forming domains of helical structures in the expanded monolayer. These domains can be seen in the TEM pictures. When the surface pressure is increased further, the area occupied by helical domains increases. This causes the separate domains to congregate and form ribs of a bilayer of molecules. A system now arose of coexisting mono- and bilayer parts. The ribs will form connections between each other under the influence of further applied surface pressure, thus forming a system consisting more and more of a bilayer of molecules. This bilayer of molecules will exist up to a pressure of about 70 mN/m when it finally collapses. This view also offered an explanation for the deviating behavior that was found during various stabilization experiments (Figure 10). In contrast with previously mentioned experiments, these experiments yielded values for the areas per repeating unit which did not agree with the pressure–area isotherms at all. The curves were S-shaped and reached a stable area of about 10 Å^2/repeating unit. We might explain this behavior by assuming that in this case a bilayer of helical molecules is formed. The difference between stabilization experiments with resulting areas corresponding to the isotherms and S-shaped curves must be sought in the presence of some kind of nucleant or condition which induces the crystallization and bilayer formation process. Once this process has started, the second layer will be formed as a co-operative process until eventually a stable bilayer of helices is formed. TEM pictures of a layer after a stabilization at 9 mN/m with an S-shaped curve agree with this point of view (Figure 11). It can

be seen clearly that structures comparable to those formed at a stabilization pressure of 20 mN/m (Figure 9d) are formed. When we take a closer look at the picture, we can even see that the structures are more homogeneous after the S-shaped curve. This can very well be explained when we take into account that the bilayer will be more perfect with increasing surface pressure in the case of a non-S-shaped stabilization. The layer stabilized at 20 mN/m thus shows large parts comparable to the homogeneous structures formed after the S-shaped curves with occasionally a few domains, as were seen in the TEM pictures of the stabilization curves at lower surface pressures.

IR on PHB at the Air–Water Interface

Figure 12 shows the results of the FT-IR reflection spectroscopy experiments compared with the calculated spectra of respectively an amorphous and a crystalline film of 1 nm thickness of PHB at the water surface. This thickness is comparable to the estimated thickness of a monolayer of PHB at the air–water interface. Comparing these two calculated spectra clearly indicates that the differences reported and described above that appear to be due to crystallinity changes are apparent here also. The experimental spectra shown between the two calculated spectra are plotted in order of decreasing area per repeating unit. The corresponding positions in the pressure–area isotherm are marked in the inset figure.

A shift of the C=O band from the amorphous toward the crystalline position can be seen with decreasing area per repeating unit. Further indications of increasing crystallinity can be extracted from the 1279 and 1185 cm^{-1} bands. The 1185 cm^{-1} band decreases in intensity with decreasing area per repeating unit whereas a band starts to appear at 1279 cm^{-1}. Both effects are strong indications that the layer at the air–water interface indeed has an increased crystalline character when the area per repeating unit decreases. This clearly confirms our theory that the transition in the isotherm is associated with a phase transition in the monolayer and that the material beyond the transition has a crystalline structure.

Conclusions

The pressure–area isotherm of PHB shows a transition which is associated with a phase transition. LB multilayers on the substrate are crystalline and show orientation, which indicates the presence of PHB in the helical conformation on the substrate. Hysteresis experiments show that irreversible changes take place during compression of the monolayer. These changes can be visualized with TEM and confirm the idea of PHB crystallizing at the air–water interface under the influence of the applied surface pressure. Occasionally occurring S-shaped stabilization curves indicate that a bilayer of helices is formed, which is in good agreement with the area found by extrapolating the linear post-transitional region of the isotherm. Infrared external reflection spectroscopy on PHB on the water surface shows that the spectral changes occurring during compression indeed match the spectral differences between amorphous and crystalline PHB.

Acknowledgment. PHB was kindly supplied by Dr. G. J. M. de Koning of the University of Eindhoven. We thank Drs. P. J. Werkman and Drs. J. G. Hagting for performing transmission electron microscopy.

References and Notes

(1) de Koning, G. J. M.; Lemstra, P. J. *Polymer* **1992**, *15*, 3292.
(2) Dawes, E. A.; Senior, P. J. *Adv. Microbiol. Physiol.* **1973**, *10*, 135.
(3) Anderson, A. J.; Dawes, E. A. *Microbiol. Rev.* **1990**, *54*, 450.
(4) Lauzier, C.; Revol, J. F.; Marchessault, R. H. *FEMS Microbiol. Rev.* **1992**, *103*, 299.
(5) Kawaguchi, Y.; Doi, Y. *FEMS Microbiol. Lett.* **1990**, *70*, 151.
(6) Lauzier, C.; Marchessault, R. H.; Smith, P.; Chanzy, H. *Polymer* **1992**, *33*, 823.
(7) Barham, P. J.; Keller, A.; Otun, E. L.; Holmes, P. A. *J. Mater. Sci.* **1984**, *19*, 2781.
(8) Barham, P. J. *J. Mater. Sci.* **1984**, *19*, 3826.
(9) Organ, S. J.; Barham, P. J. *J. Mater. Sci.* **1992**, *27*, 3239.
(10) Yokouchi, M.; Chatani, Y.; Tadokoro, H.; Teranishi, K.; Tani, H. *Polymer* **1973**, *14*, 267.
(11) Orts, W. J.; Marchessault, R. H.; Bluhm, T. L.; Hamer, G. K. *Macromolecules* **1990**, *23*, 5368.
(12) Takeda, F.; Matsumoto, M.; Takenaka, T.; Fujiyoshi, Y.; Uyeda, N. *J. Colloid Interface Sci.* **1983**, *1*, 267.
(13) Malcolm, B. R. *Proc. R. Soc.* **1968**, *A305*, 363.
(14) Brinkhuis, R. H. G.; Schouten, A. J. *Macromolecules* **1991**, *24*, 1487.
(15) Brinkhuis, R. H. G.; Schouten, A. J. *Macromolecules* **1991**, *24*, 1496.
(16) Schoondorp, M. A.; Vorenkamp, E. J.; Schouten, A. J. *Thin Solid Films* **1991**, *196*, 121.
(17) Teerenstra, M. N.; Vorenkamp, E. J.; Schouten, A. J. *Thin Solid Films* **1991**, *196*, 153.
(18) Kimura, F.; Umemera, J.; Takenaka, T. *Langmuir* **1985**, *2*, 96.
(19) Allara, D. L.; Nuzzo, R. G. *Langmuir* **1985**, *1*, 52.
(20) Allara, D. L.; Swalen, J. D. *J. Phys. Chem.* **1982**, *86*, 2700.
(21) Rabolt, J. F.; Burns, F. C.; Schlotter, N. E.; Swalen, J. D. *J. Chem. Phys.* **1983**, *78*, 946.
(22) Naselli, C.; Rabolt, J. F.; Swalen, J. D. *J. Chem. Phys.* **1985**, *82*, 2136.
(23) Orthmann, E.; Wegner, G. *Angew. Chem., Int. Ed. Engl.* **1986**, *25*, 1105.
(24) Bubeck, C.; Neher, D.; Kaltbeitzel, A.; Duda, G.; Arndt, T.; Sauer, T.; Wegner, G. *NATO ASI Ser. E* **1989**, *162*, 344.
(25) Duda, G.; Schouten, A. J.; Arndt, T.; Lieser, G.; Schmidt, G. F.; Bubeck, C.; Wegner, G. *Thin Solid Films* **1988**, *159*, 221.
(26) Bloembergen, S.; Holden, D. A.; Hamer, G. K.; Bluhm, T. L.; Marchessault, R. H. *Macromolecules* **1986**, *19*, 2865.
(27) Mielczarski, J. A. *J. Phys. Chem.* **1993**, *97*, 2649.
(28) Nobes, G. A. R.; Holden, D. A.; Marchessault, R. H. *Polymer* **1994**, *2*, 435.
(29) Yoo, K.-H.; Yu, H. *Macromolecules* **1989**, *22*, 4019.
(30) Schneider, J.; Ringsdorf, H.; Rabolt, J. F. *Macromolecules* **1989**, *22*, 205.
(31) Scheuing, D. R. *FTIR spectroscopy in colloid and interface science*; American Chemical Society: Washington, DC, 1991; Chapter 10.
(32) Scheuing, D. R. *FTIR spectroscopy in colloid and interface science*; American Chemical Society: Washington, DC, 1991; Chapter 8.
(33) Brinkhuis, R. H. G.; Schouten, A. J. *Macromolecules* **1992**, *25*, 2717.
(34) Brinkhuis, R. H. G.; Schouten, A. J. *Macromolecules* **1992**, *25*, 2732.
(35) Socrates, G. *Infrared characteristic group frequencies*; Wiley-Interscience: New York, 1980.
(36) Amor, S. R.; Rayment, T.; Sanders, J. K. M. *Macromolecules* **1991**, *24*, 4583.
(37) Allara, D. L.; Baca, A.; Pryde, C. A. *Macromolecules* **1978**, *11*, 1215.

MA945047H